Aesth Plast Surg (2023) 47:2074–2083
https://doi.org/10.1007/s00266-023-03383-2

ISAPS

ORIGINAL ARTICLE FAT INJECTION

Ultra-condensed Fat: A Novel Fat Product for Volume Augmentation

Weizi Wu[1] · Xin Bi[1] · Jing Zhao[1] · Zhousheng Lin[1] · Feng Lu[1] · Ziqing Dong[1] · Ye Li[1]

Received: 12 January 2023 / Accepted: 26 April 2023 / Published online: 25 May 2023

Abstract

Background Fat transplantation retention rate is individualized and unpredictable. The presence of blood components and oil droplets in the injected lipoaspirate increases inflammation and fibrosis in a dose-dependent manner, and is probably the key factor associated with poor retention.

Objectives This study describes a volumetric fat grafting strategy based on optimization of grafts via screening intact fat particles and absorbing free oil droplets and impurities.

Methods Centrifuged fat components were analyzed by *n*-hexane leaching. A special device was applied to de-oil intact fat components and obtain ultra-condensed fat (UCF). UCF was evaluated by scanning electron microscopy, particle size analysis, and flow cytometric analysis. Histological and immunohistochemical changes were investigated in a nude mouse fat graft model over 90 days.

Results The lower 50% of centrifuged fat was concentrated to 40% of the original volume to obtain UCF. In UCF, the free oil droplet content was less than 10%, more than 80% of particles were larger than 1000 μm, and architecturally important fat components were present. The retention rate of UCF was significantly higher than that of Coleman fat on day 90 (57.5 ± 2.7% vs. 32.8 ± 2.5%, $p < 0.001$). Histological analysis detected small preadipocytes with multiple intracellular lipid droplets on day 3 in UCF grafts, indicative of early adipogenesis. Angiogenesis and macrophage infiltration were observed in UCF grafts soon after transplantation.

Conclusion Adipose regeneration with UCF involves rapid macrophage infiltration and exit, resulting in angiogenesis and adipogenesis. UCF may serve as a lipofiller which is beneficial for fat regeneration.

Level of Evidence IV This journal requires that authors assign a level of evidence to each article. For a full description of these Evidence-Based Medicine ratings, please refer to the Table of Contents or the online Instructions to Authors http://www.springer.com/00266.

Keywords Fat grafting · Fat purification · Volume augmentation

Abbreviations

CF Coleman fat
UCF Ultra-condensed fat

Introduction

Autologous fat is considered to be a highly accessible and histocompatible tissue graft, and is widely applied in aesthetic and plastic surgery. Unfortunately, volume retention upon fat transplantation is individualized and unpredictable. The graft volume often decreases by up to 50–90% [1–3] postoperatively with a mean follow-up

Weizi Wu and Xin Bi contributed equally to this study and should be considered co-first authors.

Feng Lu and Ziqing Dong and Ye Li contributed equally to this study and should be considered co-first corresponding authors.

✉ Feng Lu
doctorlufeng@hotmail.com

✉ Ziqing Dong
doctordongziqing@outlook.com

✉ Ye Li
liyefimmu@outlook.com

[1] Department of Plastic and Cosmetic Surgery, Nanfang Hospital, Southern Medical University, 1838 Guangzhou North Road, Guangzhou 510515, Guangdong, People's Republic of China

period of 3–24 months. Fat grafting is generally repeated or over-corrected to obtain desirable results, which may result in post-operative reactive swelling and Facial Overfilled Syndrome [4, 5]. Patients desire a youthful and natural appearance without the telltale signs of any cosmetic intervention. The gap between patient expectations and the ability of fat transplantation surgeons to deliver a realistic cosmetic result is sometimes large, but an appropriate lipofiller may help to narrow this gap.

Fat processing methods [6] play a significant role in optimize fat graft survival and outcomes. The centrifugation method is based on density screening and condenses adipose-derived stem cells (ASCs) and angiogenic factors in the high-density fraction of lipoaspirate [7, 8]. The filtration method [9] is another well-accepted technique based on fat particle size screening and minimizes the false volume [10] of fat grafts, including ineffective components in the liquid phase (tumescent fluid and blood), free oil droplets, and disrupted adipocytes. The presence of blood components [11] and oil droplets [12] in the injected lipoaspirate increases inflammation and fibrosis in a dose-dependent manner, and is probably the key factor associated with poor retention and oil cyst formation after fat transplantation.

This study takes the advantages of centrifugation and filtration to design a novel purification device which remove the pseudo-volumetric components and retention of adipose particles in a suitable tissue structure. We harvested a high-quality fat product named ultra-condensed fat (UCF), and investigated the mechanism by which UCF retains volume.

Materials and Methods

Fat Harvesting

Lipoaspirate was harvested from the abdomen from human donors aged 16–60 years with body mass indices ranging from 18.3 to 31.5 kg/m^2. Donors were not excluded based on any comorbidity. After local infiltration of tumescent fluid (2% lidocaine 20 ml + epinephrine 1 mg + saline 1000 ml), the negative pressure of suction was − 0.75 ATM performed with a 3 mm multiport cannula, containing several sharp side holes 1 mm in diameter (Tulip Medical Products, San Diego, CA, USA) according to Coleman's technique [6]. After centrifugation, the liquid phase from the bottom syringe was drained and the fat component was divided into the upper 50% fat and lower 50% fat. The fat was then collected using blood bags, stored in an ice box and transported to the laboratory for less than 1 hour before each experiment.

Measurement of Centrifuged Fat Components

The leaching method uses the principle of the mutual solubility of fats and organic solvents to determine the oil ratio [13] (Supplemental Fig. 1). The upper 50% fat, lower 50% fat, and UCF were mixed with the organic solvent (*n*-hexane) respectively in a glass container at the optimal ratio (1:1 by volume). Leaching extraction using *n*-hexane involved performing a combination of mixing and centrifugation three times. The mixture was centrifuged (1200*g*, 3 min) and the bottom liquid was collected to measure the volume of the aqueous fraction. The supernatant of the centrifuged mixture was collected. The middle layer of fat was mixed with *n*-hexane and the procedure was repeated. After the third time, the supernatant was collected with a measuring cup and the volume of the fat layer was measured. The supernatant was placed in a fume hood and left for 72 h at 30 °C to allow evaporation of *n*-hexane. The volume of free oil droplets remaining after evaporation was measured.

UCF Preparation

This closed, disposable, sterile device contained oil absorption material (Fig. 1A), a 100 mesh filter bag (Fig. 1B), and liquid phase absorption materials (Fig. 1C). The oil absorption material comprised meltblown polypropylene fibers wrapped in non-woven fabric. The 100 mesh filter bag was located between the liquid phase absorption materials and oil absorption material. The liquid phase absorption materials comprised non-woven fabric filled with superabsorbent polymer granules. The materials and filter were all located in an ethylene-vinyl acetate copolymer (EVA) bag (Fig. 1D) compose the UCF processing device (Fig. 1E). After transferring the lower 50% fat (Fig. 1F) to the inner filter bag, the device was sealed and left for 5 min, the fat was carefully scraped out of the filter bag using the handle of a scalpel, and the final product was concentrated to 40% of the original volume. This purified fat was named UCF (Fig. 1G) (Supplemental Video).

Flow Cytometric Analysis

Isolated stromal vascular fractions of Coleman fat and UCF were obtained. Samples were stained with fluorescein isothiocyanate-conjugated mouse anti-human CD31, CD34, and CD45 antibodies (BD Biosciences, San Jose, USA) and analyzed by multicolor flow cytometry (LSR II, BD Biosciences). Changes in cell composition were calculated according to surface marker expression profiles. CD45−/CD31−/CD34+ and CD45−/CD31+/CD34+ cells were regarded as ASCs and endothelial cells (ECs),

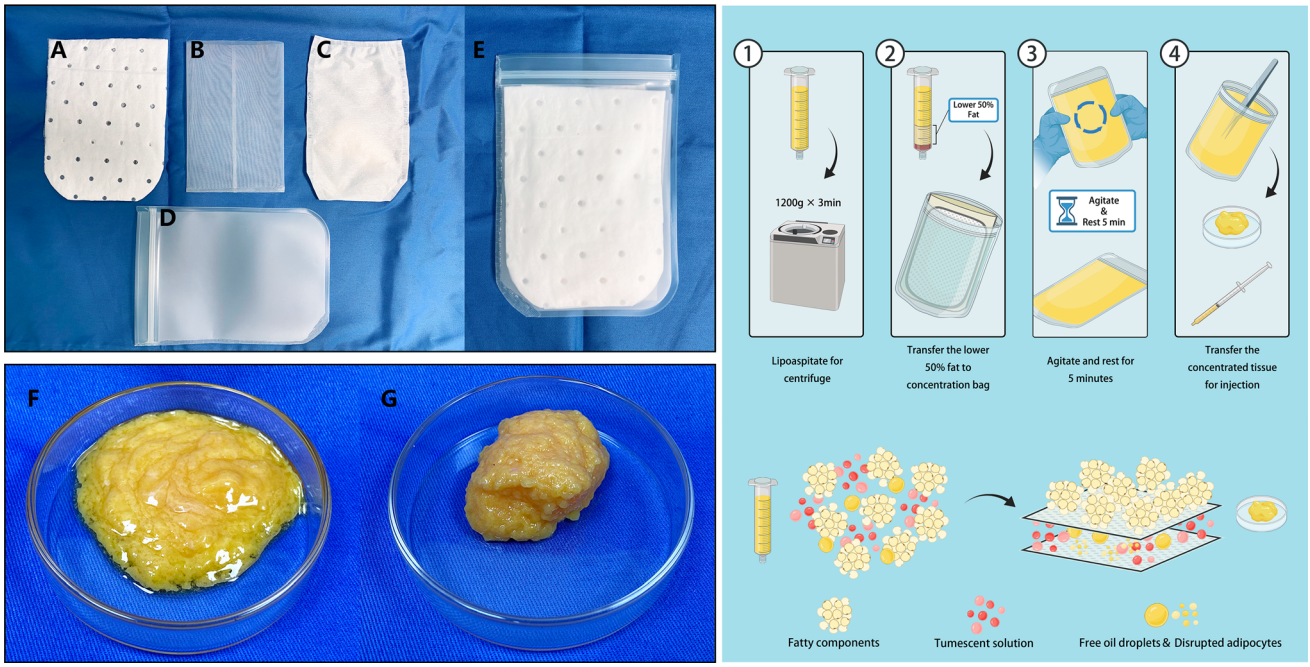

Fig. 1 The closed disposable sterile device contained oil absorption material (**A**), a 100 mesh filter bag (**B**), and liquid phase absorption materials (**C**) (*left above*). The materials and filter were all located in an ethylene-vinyl acetate copolymer (EVA) bag (**D**) compose the UCF processing device (**E**). The lower 50% fat (**F**) contained many free oil droplets, whereas UCF (**G**) contained grainy, well-defined, jelly-like adipose tissue (*left below*). Schematic showing the processing of UCF (*right*)

respectively. Their populations were determined using CellQuest Pro software (BD Biosciences).

Scanning Electron Microscopy (SEM)

Samples were fixed with 2% glutaraldehyde and 1% osmium tetroxide, dehydrated in acetone, sputtered with gold using an MED 010 coater, and examined under a S-3000N scanning electron microscope (Hitachi, Ltd., Tokyo, JPN).

Particle Size Analysis

Tissue samples were agitated in saline and loaded into the sample cup to measure particle sizes by laser diffraction particle size analyzer (Mastersizer 3000, Malvern Panalytical, Ltd, Malvern, UK). Data were plotted as a pie chart showing the distribution of particle sizes.

Nude Mouse Fat Grafting Model

Eighty-four healthy nude mice (provided by the Experimental Animal Center, Medical University) weighing 15–18 g and aged 6–8 weeks were housed in individual cages with a 12 h light/dark cycle and provided with standard food and water *ad libitum*. All animal experiments were approved by the Hospital Animal Ethics Committee Laboratory and were conducted according to the guidelines of the National Health and Medical Research Council of China. Coleman fat or UCF was grafted. In total, 0.3 ml Coleman fat or UCF was injected into dorsal subcutaneous tissues using a 1 ml syringe with a blunt infiltration cannula. At day 3, 7, 14, 30, 60, or 90 post-grafting, the grafts were harvested and their volumes were measured. The graft retention rate (%) = graft volume at harvest/injected fat volume (i.e., 0.3 ml) × 100%.

Histological Analysis

Samples were fixed in 4% paraformaldehyde, dehydrated, and embedded in paraffin for hematoxylin and eosin staining. Paraffin sections examined under an Olympus CX-31 microscope (Olympus Corp., Tokyo, Japan), and photographed using a NanoZoomer S360 digital slide scanner (Hamamatsu Photonics K.K., Hamamatsu, JPN).

Immunofluorescence Staining

Paraffin sections were stained with an anti-CD31 antibody (1:3000; Abcam, Cambridge, UK), an anti-perilipin-1

rabbit monoclonal antibody (1:100; Cell Signaling Technology, Danvers, USA), an anti-galectin 3 antibody (1:100; Abcam, Cambridge, UK), and an anti-CD206 rabbit monoclonal antibody (1:200; Cell Signaling Technology, Danvers, USA). After washing, the samples were incubated with goat anti-rabbit IgG (Abcam, ab205718, 1:4000), Alexa Fluor 488-conjugated donkey anti-rabbit IgG (1:400; Life Technologies, Eugene, USA), and Alexa Fluor 594-conjugated donkey anti-mouse IgG (1:400; Life Technologies, Eugene, USA) secondary antibodies, respectively. Nuclei were stained with DAPI (Solarbio Science & Technology, Beijing, CHN).

Quantitative Polymerase Chain Reaction (q-PCR)

Tissue samples total RNA was extracted using TRIzol Reagent (Invitrogen Life Technologies, Carlsbad, CA) according to the manufacturer's protocol. The genes of interest were amplified over 40 cycles and analyzed with an ABI PRISM 7500 Sequence Detection System and SYBR Green PCR Master Mix (Applied Biosystems, Foster City, USA). Expression levels were calculated using the 2-ΔΔCt method. The primers used are listed in Table 1.

Statistical Analysis

All data are expressed as mean ± standard deviation. Two groups were compared at single time points using the independent *t* test. Groups at all time points were compared using a one-way analysis of variance. $p < 0.05$ was considered statistically significant.

Results

Measurement of Centrifuged Fat Components

The upper 50% fat contained 37.6 ± 4.0% fatty components, 57.3 ± 4.8% oil droplets, and 4.8 ± 2.0% aqueous fraction. The lower 50% fat contained 42.9 ± 3.1% fatty components, 49.1 ± 4.5% oil droplets, and 7.8 ± 4.0% aqueous fraction. UCF contained 91.2 ± 2.0% fatty components, 4.7 ± 1.1% oil droplets, and 3.3 ± 1.3% aqueous fraction (Fig. 2). The lower 50% fat contained more fatty components and fewer free oil droplets than the upper 50% fat (Supplemental Fig. 2) (both $p < 0.001$).

Physical Properties of UCF and its Constituent Cells

SEM revealed that UCF had an intact lobular structure and contained adipocytes tightly clustered under interconnecting mesenchyme (Fig. 3A). Particle size analysis (Fig. 3B) revealed that 82.38% and 61.94% of particles were larger than 1000 μm in UCF and Coleman fat, respectively. Flow cytometry indicated that the densities of ACSs and ECs were higher in UCF than in Coleman fat ($1.6 \pm 0.03 \times 10^5$ and $7.73 \pm 0.15 \times 10^4$ cells/ml versus $5.45 \pm 0.36 \times 10^4$ and $2.58 \pm 0.08 \times 10^4$ cells/ml, respectively) (Fig. 3C) ($p < 0.001$).

Assessment of Fat Graft Retention

Quantification of graft volume indicated that the retention rate of Coleman fat remained stable from day 1 to day 14, decreased sharply from day 14 to day 30, and remained constant thereafter. By contrast, the retention rate of UCF decreased sharply from day 7 to day 14, and remained constant thereafter (Fig. 4, *above*). The retention rate of UCF was significantly higher than that of Coleman fat on days 30, 60, and 90 (all $p < 0.001$). On day 90, the retention rates of UCF and Coleman fat were 57.5 ± 2.7% and 32.8 ± 2.5%, respectively (Fig. 4, *below*).

Histological Evaluation of Fat Grafts

Small preadipocytes with multiple intracellular lipid droplets were observed in UCF grafts from day 3 to day 30 and in Coleman fat grafts from day 7 to day 30. On day 30,

Table 1 Primer sequences used for quantitative polymerase chain reaction

Gene	Primer sequences
Interleukin-6 (IL-6)	Forward: 5′-TGCAATAACCACCCCTGACC-3′
	Reverse: 5′-GTGCCCATGCTACATTTGCC-3′
Interleukin-8 (IL-8)	Forward: 5′-TACTCCCAGTCTTGTCATTGCC-3′
	Reverse: 5′-ATTGACTGTGGAGTTTTGGCTG-3′
Interleukin-10 (IL-10)	Forward: 5′-AAGCCTGACCACGCTTTCTA-3′
	Reverse: 5′-CTCCGAGACACTGGAAGGTG-3′
Tumor necrosis factor-α (TNF-α)	Forward: 5′-AGAACTCACTGGGGCCTACA-3′
	Reverse: 5′-GCTCCGTGTCTCAAGGAAGT-3′
β-actin	Forward: 5′-GTCACCAACTGGGACGACAT-3′
	Reverse: 5′-TAGCAACGTACATGGCTGGG-3′

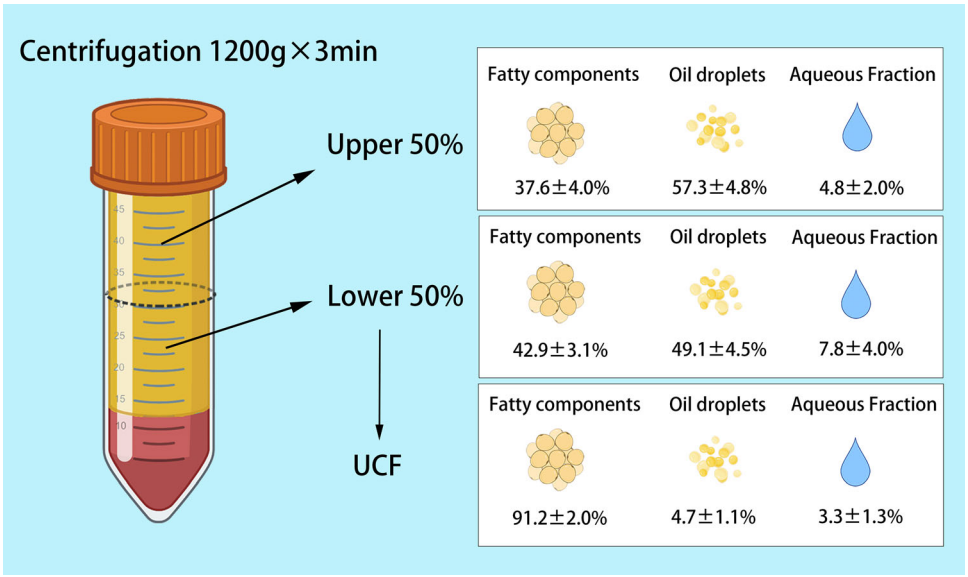

Fig. 2 The upper 50% fat contained 37.6 ± 4.0% fatty components, 57.3 ± 4.8% oil droplets, and 4.8 ± 2.0% aqueous fraction. The lower 50% fat contained 42.9 ± 3.1% fatty components, 49.1 ± 4.5% oil droplets, and 7.8 ± 4.0% aqueous fraction. UCF contained 91.2 ± 2.0% fatty components, 4.7 ± 1.1% oil droplets, and 3.3 ± 1.3% aqueous fraction. The lower 50% fat contained more fatty components, fewer free oil droplets, and a larger aqueous fraction that the upper 50% fat

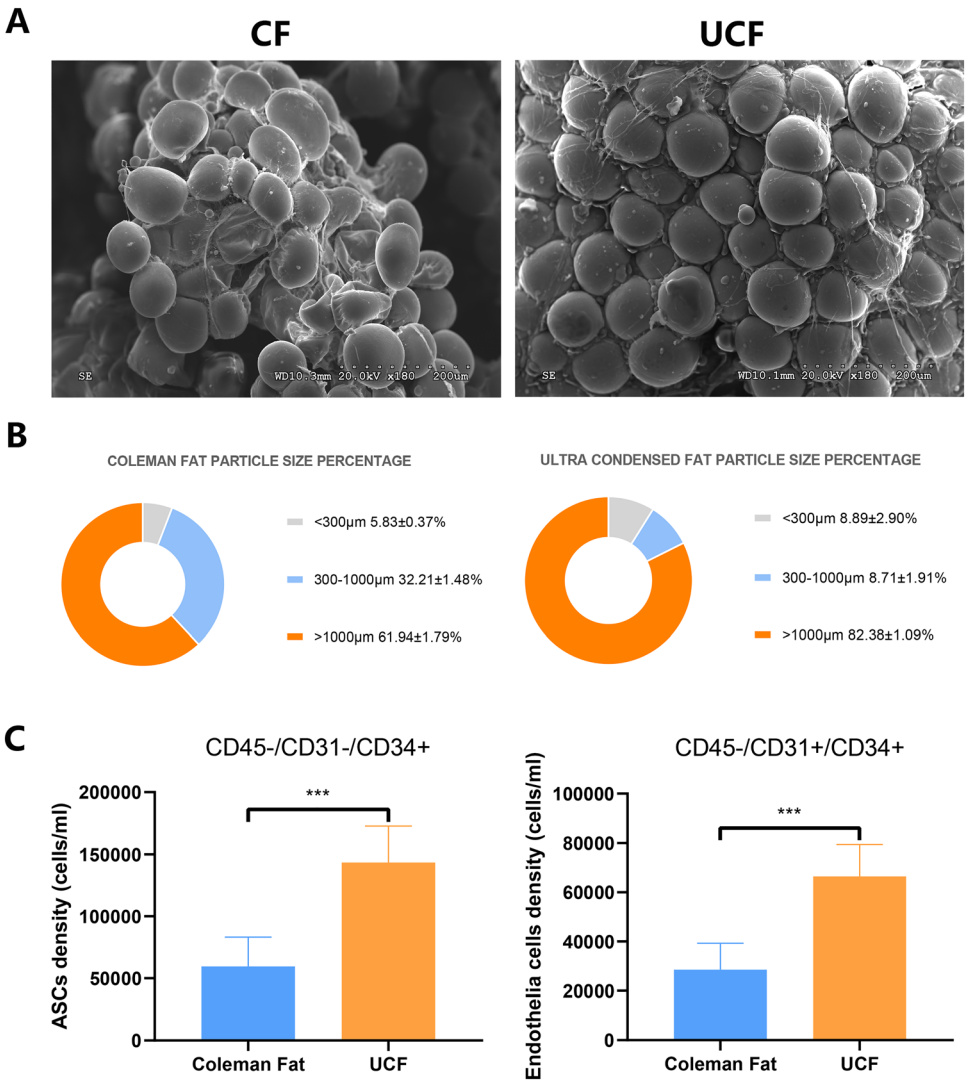

Fig. 3 Structural comparison of Coleman fat (**A left**) and UCF (**A right**) by SEM. Coleman fat contained a large volume of loosely connected adipocytes, whereas UCF contained intact adipocytes tightly connected in the extracellular matrix. *Scale bar* = 200 μm. Fat particle size analysis using a laser diffraction particle size analyzer showed that 82.38% and 61.94% of particles were larger than 1000 μm in UCF and Coleman fat, respectively (**B**). Flow cytometry indicated that the densities of ACSs and ECs were higher in UCF than in Coleman fat ($1.6 \pm 0.03 \times 10^5$ and $7.73 \pm 0.15 \times 10^4$ cells/ml versus $5.45 \pm 0.36 \times 10^4$ and $2.58 \pm 0.08 \times 10^4$ cells/ml, respectively) (*C*) (***$p < 0.001$) ($n = 7$)

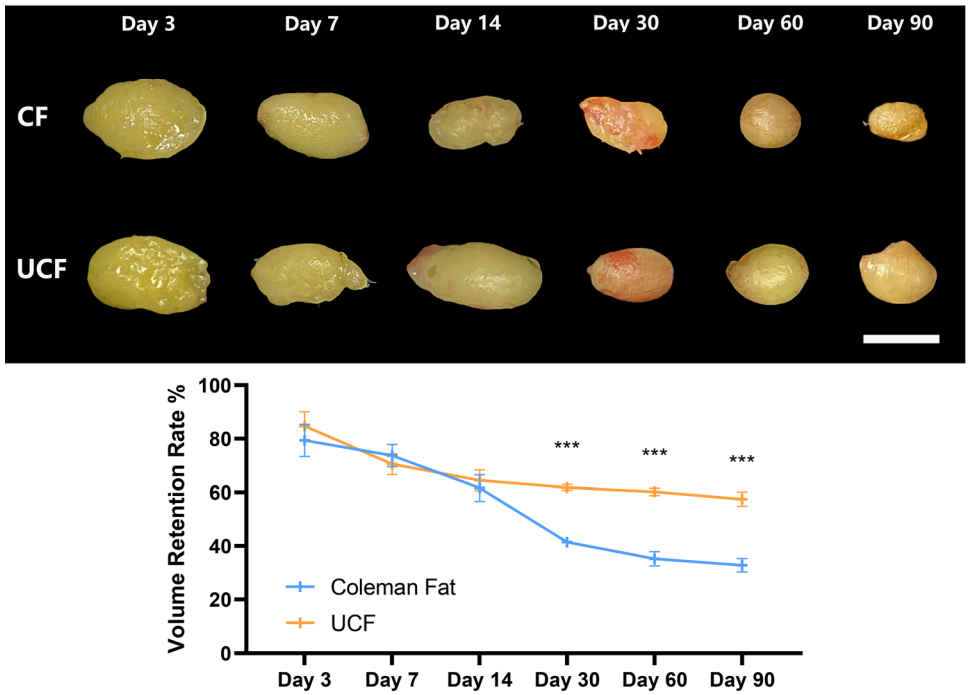

Fig. 4 Representative volume changes of grafts *in vivo* (*above*). *Scale bar* = 1 cm. Quantification of graft volume from day 3 to day 90 (*below*) (*$p < 0.05$; **$p < 0.01$; ***$p < 0.001$) ($n = 7$)

UCF grafts contained more preadipocytes and fewer inflammatory cells than Coleman fat grafts. On day 60, oil cysts were observed in most Coleman fat grafts. On day 90, both UCF and Coleman fat grafts exhibited a normal adipose tissue structure, but Coleman fat grafts contained larger oil cysts (Fig. 5).

Adipogenesis and Angiogenesis in Fat Grafts

The perilipin+ area shrank on day 7 and was regenerated on day 14 in UCF grafts, and shrank on day 14 and was regenerated on day 30 in Coleman fat grafts. Small preadipocytes were observed from day 3 to day 60 in UCF grafts, and from day 7 to day 60 in Coleman fat grafts (Fig. 6A). On days 7, 14, 30, 60, and 90, there were significantly more perilipin+ cells in UCF grafts than in Coleman fat grafts ($p < 0.01$). The number of CD31+ cells peaked on days 7 and 14 in UCF and Coleman fat grafts, respectively. On days 7, 14, and 30, there were significantly more CD31+ cells in UCF grafts than in Coleman fat grafts (Fig. 6B). ($p < 0.01$).

Macrophage Infiltration of Fat Grafts

M1 (MAC2+/CD206-) macrophages infiltrated UCF and Coleman fat grafts on days 3 and 7, respectively. M2 (MAC2+/CD206+) macrophages were observed in UCF and Coleman fat grafts on days 7 and 14, respectively, indicating that M2 polarization occurred earlier in UCF than in Coleman fat (Fig. 7A). The number of M1 (MAC2+/CD206-) macrophages in UCF grafts peaked on day 7 and was significantly higher than that in Coleman fat grafts on days 3 ($p < 0.01$), 7 ($p < 0.001$), 14 ($p < 0.01$), 30 ($p < 0.05$), and 90 ($p < 0.01$). The number of M2 (MAC2+/CD206+) macrophages in UCF grafts peaked on day 7 and was significantly higher than that in Coleman fat grafts on days 3 ($p < 0.01$), 7 ($p < 0.001$), 30 ($p < 0.01$), 60 ($p < 0.05$), and 90 ($p < 0.01$) (Fig. 7B). The

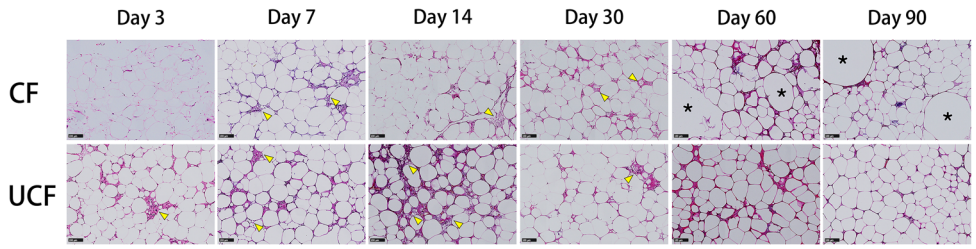

Fig. 5 Histological comparison of grafts by hematoxylin and eosin staining from day 3 to day 90. Small adipocytes with multiple intracellular lipid droplets are indicated by yellow triangles. Oil cysts are indicated by asterisks. *Scale bar* = 100 μm; ($n = 7$)

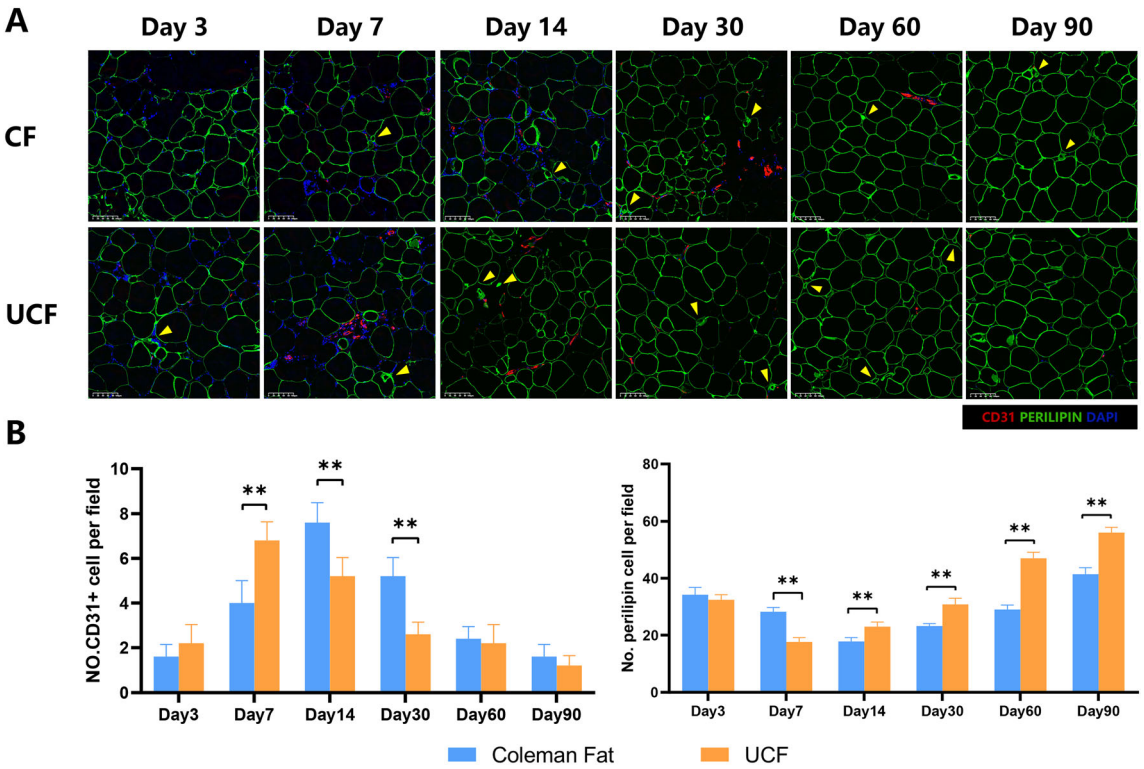

Fig. 6 Comparison of grafts by immunofluorescence staining from day 3 to day 90. Small preadipocytes are indicated by yellow triangles (*above*). *Scale bar* = 1 cm. Quantification of CD31+ and perilipin+ cells in grafts from day 3 to day 90 (*below*) (*$p < 0.05$; **$p < 0.01$; ***$p < 0.001$); ($n = 7$)

proinflammatory cytokines IL-6, TNF-α mRNA, and IL-8 levels peaked on day 7 and decreased on day 14 in UCF grafts, and peaked on day 14 and declined over the following days in Coleman fat grafts. The anti-inflammatory cytokine IL-10 mRNA levels peaked on day 7 and decreased on day 14 in UCF grafts, and peaked on day 14 and declined over the following days in Coleman fat grafts. The IL-6, TNF-α, IL-8, and IL-10 levels were significantly higher in UCF grafts than in Coleman fat grafts from day 3 to day 90[IL-6: days 3 ($p < 0.01$), 7 ($p < 0.01$), 14 ($p < 0.01$), 30 ($p < 0.001$), 60 ($p < 0.01$), and 90 ($p < 0.01$); TNF-α: days 3 ($p < 0.01$), 7 ($p < 0.01$), 14 ($p < 0.01$), 30 ($p < 0.01$), 60 ($p < 0.01$), and 90 ($p < 0.05$); IL-8: all $p < 0.01$; IL-10: all $p < 0.01$] (Fig. 7C).

Discussion

This study presents a novel strategy to screen intact adipocytes using a combination of centrifugation and filtration fat purification methods. UCF was prepared from the lower 50% fat contained with more fatty components, fewer free oil droplets. Macroscopically, UCF contained grainy, well-defined, jelly-like adipose tissue. SEM demonstrated that UCF had a lobular structure and contained adipocytes. In total, 82.38% of particles were larger than 1000 μm in UCF, similar to commercial products such as REVOLVE and PureGraft [14]. ASCs and ECs were concentrated in UCF. According to these results, we specify that (1) UCF should be concentrated to 40% of the original volume, (2) UCF should have a free oil droplet content of less than 10%, and (3) more than 80% of particles in UCF should be larger than 1000 μm.

Our purification device screens the highest quality fat particles in lipoaspirates and removes non-essential components, while medical oil-absorbing fibers absorb free oil droplets, thereby reducing the false volume. This processing method is inexpensive (PureGraft 850 costs 450€) and efficient. Approximately 120 ml fat is processed in 5 min using this method, compared with 60 ml fat using Telfa-rolling [15]. Additionally, classic purification methods rarely focus on removal of oil droplets. Fat granules are not present in native adipose tissue, but form during the harvesting step. Under shear force [16], adipose tissue is divided into intact globules and crushed particles, which produce free oil in lipoaspirates. In the early stage after transplantation, oil released by damaged adipocytes together with free oil droplets may increase inflammation with abnormal infiltration of leukocytes and cytokine production, and thereby aggravate the burden in the recipient area,

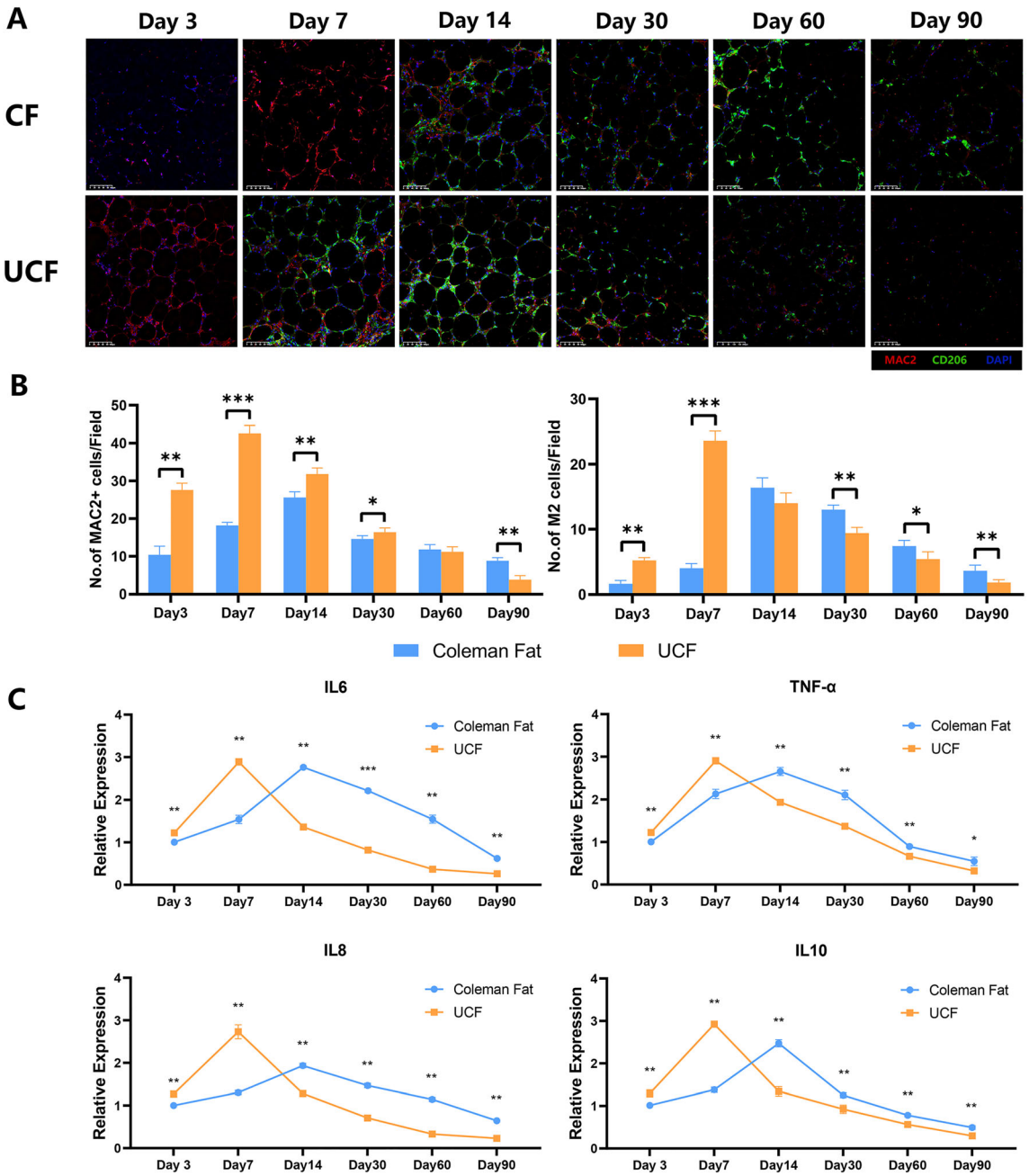

Fig. 7 Comparison of macrophage infiltration between grafts by immunofluorescence staining (**A**). *Scale bar* = 100 μm. Quantitative analysis of MAC2+ macrophages from day 3 to day 90 (**B**) (*$p < 0.05$; **$p < 0.01$; ***$p < 0.001$). Expression of IL-6, TNF-α, IL-8, and IL-10 mRNAs in fat grafts(*below*) (*$p < 0.05$; **$p < 0.01$; ***$p < 0.001$). The number of M1 (MAC2+/CD206-) macrophages in UCF grafts peaked on day 7 and was significantly higher than that in Coleman fat grafts on days 3 ($p < 0.01$), 7 ($p < 0.001$), 14 ($p < 0.01$), 30 ($p < 0.05$), and 90 ($p < 0.01$). The number of M2 (MAC2+/CD206+) macrophages in UCF grafts peaked on day 7 and was significantly higher than that in Coleman fat grafts on days 3 ($p < 0.01$), 7 ($p < 0.001$), 30 ($p < 0.01$), 60 ($p < 0.05$), and 90 ($p < 0.01$). The expression levels of mRNAs encoding four potent inflammatory cytokines, interleukin-6 (IL-6), tumor necrosis factor-α (TNF-α), interleukin-8 (IL-8), and interleukin-10 (IL-10), were compared between the grafts by q-PCR (*C*). The IL-6, TNF-α, IL-8, and IL-10 levels were significantly higher in UCF grafts than in Coleman fat grafts from day 3 to day 90 [IL-6: days 3 ($p < 0.01$), 7 ($p < 0.01$), 14 ($p < 0.01$), 30 (p < 0.001), 60 ($p < 0.01$), and 90 ($p < 0.01$); TNF-α: days 3 ($p < 0.01$), 7 ($p < 0.01$), 14 ($p < 0.01$), 30 ($p < 0.01$), 60 ($p < 0.01$), and 90 ($p < 0.05$); IL-8: all $p < 0.01$; IL-10: all $p < 0.01$] ($n = 7$)

leading to fibrotic repair or oil cyst formation. Stromal vascular fraction-gel [17] is produced by mechanical emulsification and removes oil, and has satisfactory adipogenic and angiogenic effects in our experience. This indirectly illustrates that oil negatively affects fat grafting. Fat lobules have two extracellular matrices, namely, septa

and stroma, which define the niches of CD45−/CD34+/CD31− progenitor cells [18]. It is of prime importance to recognize that fat particles integrity defined as intact globules of adipocytes and interconnecting mesenchymal that serve as the reservoir responsible for tissue repair and regeneration. Thus, structurally intact fat particles are vital for fat grafting.

Macrophages rapidly infiltrated and exited UCF grafts, contributing to graft volume retention. Infiltration of M1 (MAC2+/CD206-) macrophages started on day 3, peaked on day 7, and decreased on day 30 in UCF grafts. Additionally, the level of M2 (MAC2+/CD206+) macrophages peaked on day 7 and they became the dominant macrophages in UCF grafts. That indicated that the adipose tissue repairing from inflammation phase into regeneration phase. Upregulation of the proinflammatory cytokines IL-6, TNF-α and IL-8 verifies the activation status of M1 macrophages at the molecular level. Upregulation of the anti-inflammatory cytokines IL-10 verifies the activation status of M2 macrophages at the molecular level. M1 and M2 macrophages showed almost identical trends, suggesting a timely balance between pro-inflammation and anti-inflammation. This balance promotes graft regeneration [19]. However, long-term chronic inflammation is tightly connected with fibrosis and oil cyst formation [20]. On the other hand, the balance indirectly manifested the intact fat particles have healthy immune regulation capacity and regeneration ability. Therefore, we consider that removal of free oil droplets or impurities and retention of as many intact adipose granules as possible are crucial to maximize the longevity of fat grafts.

In UCF grafts, the number of CD31+ cells peaked on day 7 and vascularization was better than in Coleman fat grafts. Hematoxylin and eosin staining and immunofluorescence staining for perilipin revealed that small adipocytes with multiple lipid droplets emerged early in UCF grafts *in vivo*. Angiogenesis and inflammation are mutually supportive processes. Several studies have demonstrated that monocytes/macrophages contribute to angiogenesis via a variety of mechanisms including secretion of vascular endothelial growth factor and other cytokines, promote intima regeneration, and contribute to collateral growth under hypoxic conditions [21–23]. Early infiltration of macrophages induces vascularization and promotes fat regeneration [24, 25]. These results illustrate the potential regenerative capacity of UCF in terms of wide clinical application.

There are many methods to deal with fat tissue, such as microfat and nanofat. Compared to microfat and nanofat, UCF removes oil but retains a more complete Coleman structure. Similar to microfat and nanofat, UCF also promote inflammation, vascularization, and tissue regeneration after transplantation. However, microfat and nanofat are suitable for fine filling because of their small size. UCF is more suitable for relatively large volume of tissue filling [26, 27]. There also limitations in this study. Firstly, in the concentration of fat tissue, donors were not excluded based on any comorbidity. In practical clinical applications, the differences between different individuals may require further practice to verify. Therefore, the second point is that UCF still needs clinical use to verify its effectiveness in various aspects. In fact, we have already initiated clinical trials, and in the following studies, we will demonstrate the clinical comparison between UCF and Coleman fat.

Conclusion

Regeneration of UCF involves rapid infiltration and exit of macrophages, resulting in high-quality angiogenesis and adipogenesis. UCF may serve as a lipofiller which is beneficial for fat regeneration.

Funding This work was supported by the National Natural Science Foundation of China (82072197), and the Science and Technology Innovation Plan of Hunan Province (2018SK50703).

Declarations

Conflict of interest The authors declare that they have no conflicts of interest to disclose.

Statement of Human and Animal Rights, or Ethical Approval All animal experiments were approved by the Institutional Animal Care and Use Committee of Nanfang Hospital and were conducted in accordance with the guidelines of the National Health and Medical Research Committee (People's Republic of China). And all applicable institutional and national guidelines for the care and use of animals were followed.

Informed Consent For this type of study informed consent is not required.

References

1. Coleman SR, Katzel EB (2015) Fat grafting for facial filling and regeneration. Clin Plast Surg 42:289–300
2. Schultz KP, Raghuram A, Davis MJ et al (2020) Fat grafting for facial rejuvenation. Semin Plast Surg 34:30–37
3. Lv Q, Li X, Qi Y et al (2021) Volume retention after facial fat grafting and relevant factors: a systematic review and meta-analysis. Aesthet Plast Surg. 45:506–520
4. Cotofana S, Gotkin RH, Frank K et al (2020) Anatomy behind the facial overfilled syndrome: the transverse facial septum. Dermatol Surg 46:e16–e22
5. Corduff N, Juniarti L, Lim TS (2022) Current practices in hyaluronic acid dermal filler treatment in asia pacific and practical approaches to achieving safe and natural-looking results. Clin Cosmet Investig Dermatol 15:1213–1223

6. Strong AL, Cederna PS, Rubin JP et al (2015) The current state of fat grafting: a review of harvesting, processing, and injection techniques. Plast Reconstr Surg 136:897–912
7. Allen RJ, Canizares O, Scharf C et al (2013) Grading lipoaspirate. Plast Reconstr Surg 131:38–45
8. Guan J, He Y, Wang X et al (2020) Identification of high-quality fat based on precision centrifugation in lipoaspirates using marker floats. Plast Reconstr Surg 146:541–550
9. Kaur S, Rubin JP, Gusenoff J et al (2022) The general registry of autologous fat transfer: concept, design, and analysis of fat grafting complications. Plast Reconstr Surg 149:1118e–1129e
10. Pinto H, Fontdevila J (2019) Regenerative medicine procedures for aesthetic physicians. Springer, Cham
11. Jin S, Yang Z, Han X et al (2021) Blood impairs viability of fat grafts and adipose stem cells: importance of washing in fat processing. Aesthet Surg J 41:86–97
12. Tynan GA, Hearnden CH, Oleszycka E et al (2014) Endogenous oils derived from human adipocytes are potent adjuvants that promote IL-1alpha-dependent inflammation. Diabetes 63:2037–2050
13. Uhm JT, Yoon WB (2011) Effects of high-pressure process on kinetics of leaching oil from soybean powder using hexane in batch systems. J Food Sci 76:E444–E449
14. Fang C, Patel P, Li H, et al. (2020) Physical, biochemical, and biologic properties of fat graft processed via different methods. Plastic and Reconstructive Surgery - Global Open
15. Del Vecchio D, Rohrich RJ (2012) A classification of clinical fat grafting. Plast Reconstr Surg 130:511–522
16. James IB, Bourne DA, DiBernardo G et al (2018) The architecture of fat grafting II. Plast Reconstr Surg 142:1219–1225
17. Yao Y, Cai J, Zhang P et al (2018) Adipose stromal vascular fraction gel grafting: a new method for tissue volumization and rejuvenation. Dermatol Surg 44:1278–1286
18. Estève D, Boulet N, Belles C, et al (2019) Lobular architecture of human adipose tissue defines the niche and fate of progenitor cells. Nat Commun 2019
19. Muñoz-Cánoves P, Serrano AL (2015) Macrophages decide between regeneration and fibrosis in muscle. Trends Endocrinol Metab 26:449–450
20. Mineda K, Kuno S, Kato H et al (2014) Chronic inflammation and progressive calcification as a result of fat necrosis: the worst outcome in fat grafting. Plast Reconstr Surg 133:1064–1072
21. Getzin T, Krishnasamy K, Gamrekelashvili J et al (2018) The chemokine receptor CX3CR1 coordinates monocyte recruitment and endothelial regeneration after arterial injury. Embo Mol Med 10:151–159
22. Corliss BA, Azimi MS, Munson JM et al (2016) Macrophages: an inflammatory link between angiogenesis and lymphangiogenesis. Microcirculation 23:95–121
23. Yang Y, Guo Z, Chen W et al (2021) M2 Macrophage-derived exosomes promote angiogenesis and growth of pancreatic ductal adenocarcinoma by targeting E2F2. Mol Ther 29:1226–1238
24. Eelen G, Treps L, Li X et al (2020) Basic and therapeutic aspects of angiogenesis updated. Circ Res 127:310–329
25. Cai J, Feng J, Liu K et al (2018) Early macrophage infiltration improves fat graft survival by inducing angiogenesis and hematopoietic stem cell recruitment. Plast Reconstr Surg 141:376–386
26. Trotzier C, Sequeira I, Auxenfans C et al (2023) Fat graft retention: adipose tissue, adipose-derived stem cells, and aging. Plast Reconstr Surg 151:420e–431e
27. Yang Z, Dong L, Jin S et al (2023) Comparison of microfat, nanofat and extracellular matrix/stromal vascular fraction gel for skin rejuvenation: basic animal research. Aesthet Surg J sjad058